arXiv:1611.05307v1 [cond-mat.stat-mech] 16 Nov 2016

A traffic model with an absorbing-state phase transition

M. L. L. Iannini,* and Ronald Dickman,†

Departamento de Física and National Institute

of Science and Technology for Complex Systems,

ICEx, Universidade Federal de Minas Gerais,

C. P. 702, 30123-970 Belo Horizonte, Minas Gerais - Brazil

(Dated: November 17, 2016)

Abstract

We consider a modified Nagel-Schreckenberg (NS) model in which drivers do not decelerate if their speed is smaller than the headway (number of empty sites to the car ahead). (In the original NS model, such a reduction in speed occurs with probability p, independent of the headway, as long as the current speed is greater than zero.) In the modified model the free-flow state (with all vehicles traveling at the maximum speed, v_{max}) is *absorbing* for densities ρ smaller than a critical value $\rho_c = 1/(v_{max} + 2)$. The phase diagram in the $\rho - p$ plane is reentrant: for densities in the range $\rho_{c,<} < \rho < \rho_c$, both small and large values of p favor free flow, while for intermediate values, a nonzero fraction of vehicles have speeds $< v_{max}$. In addition to representing a more realistic description of driving behavior, this change leads to a better understanding of the phase transition in the original model. Our results suggest an unexpected connection between traffic models and stochastic sandpiles.

PACS numbers:

Keywords:

* email: lobao@div.cefetmg.br

† email: dickman@fisica.ufmg.br

I. INTRODUCTION

The Nagel-Schreckenberg (NS) model holds a central position in traffic modeling via cellular automata, because it reproduces features commonly found in real traffic, such as the transition between free flow to jammed state, start-and-stop waves, and shocks (due to driver overreaction). This simple model represents the effect of fluctuations in driving behavior by incorporating a stochastic element: the spontaneous reduction of velocity with probability p.

Although the NS model has been studied extensively, the nature of the transition between free and jammed flow, in particular, whether it corresponds to a critical point, remains controversial [2–5]. Modifications in update rules of the NS model have been found to result in a well defined phase transition [6]. Krauss *et al.* [7] proposed a generalized version of the NS model and showed numerically that free- and congested-flow phases may coexist. While the NS model does not exhibit metastable states, which are important in observed traffic flow, including a slow-to-start rule, such that acceleration of stopped or slow vehicles is delayed compared to that of moving or faster cars, can lead to metastability [8–10]. Takayasu and Takayasu [8] were the first to suggest a cellular automaton (CA) model with a slow-to-start rule. Benjamin, Johnson, and Hui introduced a different slow-to-start rule in Ref. [9], while Barlovic *et al.* suggested a velocity-dependent randomization model [10]. Other models with metastable states are discussed in Refs. [11, 12]. A review of CA traffic models is presented in Ref. [13].

In the original NS model, at each time step (specifically, in the reduction substep), a driver with nonzero velocity reduces her speed with probability p. Here we propose a simple yet crucial modification, eliminating changes in speed in this substep when the distance to the car ahead is greater than the current speed. We believe that this rule reflects driver behavior more faithfully than does the original reduction step, in which drivers may decelerate for no apparent reason. While one might argue that distractions such as cell phones cause drivers to decelerate unnecessarily, we can expect that highways will be increasingly populated by driverless vehicles exhibiting more rational behavior. The modified model, which we call the absorbing Nagel-Schreckenberg (ANS) model, exhibits a line of absorbing-state phase transitions between free and congested flow in the $\rho - p$ plane. (Here ρ denotes the *density*, i.e., the number of vehicles per site.) The modification proposed here allows us to understand

the nature of the phase transition in the original model, and to identify a proper order parameter. The ANS model exhibits a surprising reentrant phase diagram.

Regarding the nature of the phase transition in the original NS model, the key insight is that, for $p = 0$, it exhibits a transition between an absorbing state (free flow) and an active state (congested flow) at density $\rho = 1/(v_{max} + 1)$, where v_{max} denotes the maximum speed. Free flow is absorbing because each car advances the same distance in each time step, so that the configuration simply executes rigid-body motion (in the co-moving frame it is frozen). Congested flow, by contrast, is active in the sense that the distances between vehicles change with time. Below the critical density, activity (if present initially) dies out, and an absorbing configuration is reached; above the critical density there must be activity, due to lack of sufficient space between vehicles. Setting $p > 0$ in the original model is equivalent to including a *source* of spontaneous activity. Since such a source eliminates the absorbing state [15], the original NS model *does not possess a phase transition for* $p > 0$. (It should nonetheless be possible to observe scaling phenomena as $p \to 0$.) A similar conclusion was reached by Souza and Vilar [5], who drew an analogy between the phase transition at $p = 0$ and a quantum phase transition at temperature $T = 0$. In their analogy, $p > 0$ corresponds to $T > 0$, for which, *sensu stricto*, there is again no phase transition.

The remainder of this paper is organized as follows. In the next section we define the ANS model, pointing out how it differs from the original NS model. In Sec. III we explain qualitatively the nature of the phase diagram, and report simulation results for the phase boundary. Sec. IV presents results on critical behavior, followed in Sec. V by a summary and discussion of our findings.

II. MODEL

The NS model and its absorbing counterpart (ANS) are defined on a ring of L sites, each of which may be empty or occupied by a vehicle with velocity $v = 0, 1, ..., v_{max}$. (Unless otherwise noted, we use $v_{max} = 5$, as is standard in studies of the NS model.) The dynamics, which occurs in discrete time, conserves the number N of vehicles; the associated intensive control parameter is $\rho = N/L$. Denoting the position of the i-th vehicle by x_i, we define the headway $d_i = x_{i+1} - x_i - 1$ as the number of empty sites between vehicles i and $i + 1$. Each time step consists of four substeps, as follows:

- Each vehicle with $v_i < v_{max}$ increases its velocity by one unit: $v_i \to v_i + 1$
- Each vehicle with $v_i > d_i$ reduces its velocity to $v_i = d_i$.
- NS model: each vehicle reduces its velocity by one unit with probability p.
  ANS model: each vehicle with $v_i = d_i$ reduces its velocity by one unit with probability p.
- All vehicles advance their position in accord with their velocity.

In practice, given the velocities v_i and headways d_i, there is no need to keep track of positions: the final substep is simply $d_i \to d_i - v_i + v_{i+1}$ for $i = 1, ..., N-1$, and $d_N \to d_N - v_N + v_1$.

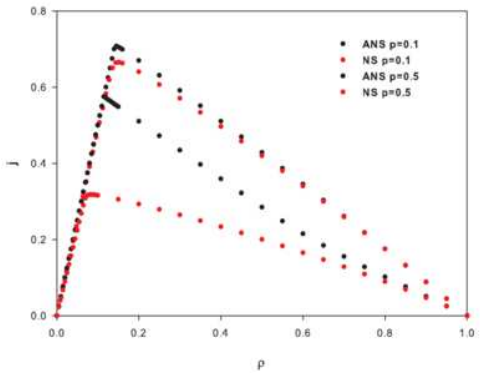

FIG. 1: (Color online) Flux j versus density in the NS and ANS models for probabilities $p = 0.1$ (upper) and $p = 0.5$ (lower). System size $L = 10^5$; vehicles are distributed randomly at $t = 0$. Error bars are smaller than symbols.

The modification of the third substep leads to several notable changes in behavior, as reflected in the fundamental diagram shown in Fig. 1. Evidently, there is a phase transition in the ANS model for $p > 0$, while there is none in the NS model. The flux q generally takes its maximum value at the transition. (For small p, however, maximum flux occurs at a density above $\rho_c = 1/(v_{max} + 2)$, approaching $\rho = \frac{1}{v_{max}+1}$ for $p = 0$). The low-density, absorbing phase has $v_i = v_{max}$ and $d_i \geq v_{max} + 1$, $\forall i$; in this phase all drivers advance in a deterministic manner, with the flux given by $J = \rho v_{max}$. In the active state, by contrast, a nonzero fraction of vehicles have $d_i \leq v_{max}$. For such vehicles, changes in velocity are possible, and the configuration is nonabsorbing. The stationary fluxes in the NS and ANS models differ significantly over a considerable interval of densities, especially for high values

of p. Below the critical density ρ_c, this difference is due the existence of an absorbing phase in the ANS model. For densities slightly above ρ_c, most vehicles have velocity $v_i = v_{max}$ and $d_i = v_{max} + 1$, although there is no absorbing state. As the density approaches unity, the differences between the fluxes in the ANS and NS models become smaller.

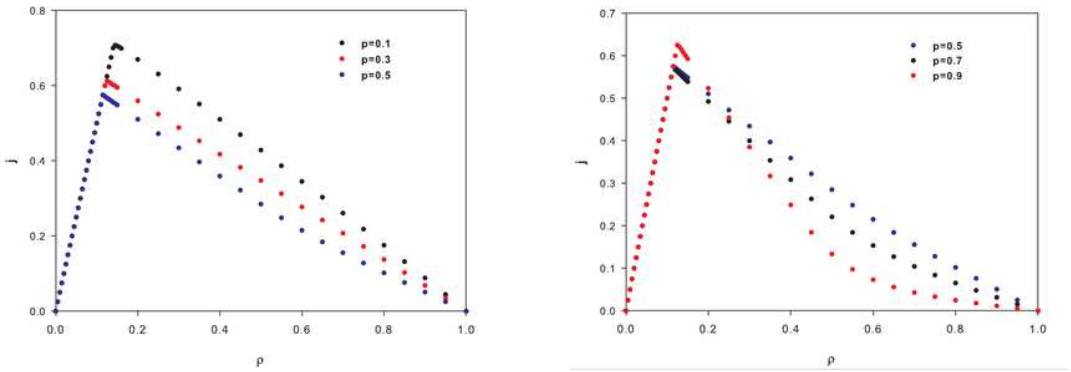

(a) (b)

FIG. 2: Flux versus density in the ANS model for (a) $p = 0.1$, 0.3 and 0.5, and (b) $p = 0.5$, 0.7 and 0.9. Note that the density of maximum flux first decreases, and then increases, with increasing p; the minimum occurs near $p \simeq 0.5$. System size $L = 10^5$; error bars are smaller than symbols.

For fixed deceleration probability p, the flux $j = \rho\overline{v}$ first grows, and then decreases as we increase the vehicle density ρ. An intriguing feature is the dependence of the density at maximum flux on the probability p: Fig. 2 shows that the density at maximum flux decreases with increasing p until reaching a minimum near $p = 0.5$, and subsequently increases with increasing p. This reflects the reentrant nature of the phase diagram, as discussed in Sec. III.

A. Special cases: $p = 0$ and $p = 1$

For the extreme values $p = 0$ and $p = 1$ the ANS model is deterministic; these two cases deserve comment. For $p = 0$, the NS and ANS models are identical. The system reaches an absorbing state, $v_i = v_{max}$, $\forall i$, for densities $\rho \leq 1/(v_{max}+1)$. For higher densities we observe nonzero activity in the steady state. We note however that there are special configurations, in which $v_i = d_i$, $\forall i$, with some $v_i < v_{max}$, whose evolution corresponds to a rigid rotation of the pattern. (A simple example is $v_i = d_i = n$, $\forall i$, with $n = 1$, 2, 3 or 4, and density $\rho = 1/(n + 1)$.) Since our interest here is in the model with $0 < p < 1$ we do not comment further on such configurations.

For the NS model with $p = 1$, from one step to the next, each velocity v_i is nonincreasing. (Of course $v_i \to v_i + 1$ at the acceleration substep, but this is immediately undone in the subsequent substeps.) Thus if the evolution leads to a state in which even one vehicle has velocity zero, all vehicles eventually stop. Such an event is inevitable for $\rho > 1/3$, since in this case $d_i \leq 1$ for at least one vehicle, which is obliged to have $v_i = 0$ after one step. For $\rho \leq \frac{1}{3}$, steady states with nonzero flux are possible, depending on the choice of initial condition. Such configurations are *metastable* in the sense that the stationary state depends on the initial distribution. In the ANS model with $p = 1$ the mean velocity in steady state is zero only for $\rho \geq 1/2$. For $\rho \leq 1/(v_{max} + 2)$, we find that the system always reaches an absorbing configuration with $\overline{v} = v_{max}$. In the remaining interval, $1/(v_{max} + 2) < \rho \leq 1/2$, we find $\overline{v} = 1 - 2\rho$.

III. PHASE DIAGRAM

A. Initial condition dependence

In studies of traffic, states are called *metastable* if they can be obtained from some, but not all initial conditions [8–12]; such states are an essential component of real traffic. Since the NS model is not capable of reproducing this feature, models with modified update rules have been investigated by several authors [8–10]. In the ANS model, by contrast, there is a region in the $\rho - p$ plane in which, depending on the initial condition, the system may evolve to an active state or an absorbing one. Our results are consistent with the usual scenario for absorbing-state phase transitions [15–17]: activity in a finite system has a finite lifetime; in the active phase, however, the mean lifetime diverges as the system size tends to infinity. Properties of the active phase may be inferred from simulations that probe the *quasistationary regime* of large but finite systems [18].

To verify the existence of metastable states in the ANS model, we study its evolution starting from two very different classes of initial conditions (ICs): homogeneous and jammed. In a homogeneous IC, the headways d_i are initially are uniform as possible, given the density $\rho = 1/(1+\overline{d})$, where $\overline{d}$ denotes the mean headway. In this case the initial velocity is v_{max} for all vehicles. In a jammed IC, N vehicles occupy the N contiguous sites, while the remaining $N(\rho^{-1} - 1)$ sites are vacant; in this case $d_i = 0$ for $i = 1, ..., N - 1$, and only vehicle N has

a nonzero initial velocity ($v_N = v_{max}$). Homogeneous ICs are much closer to an absorbing configuration than are jammed ICs.

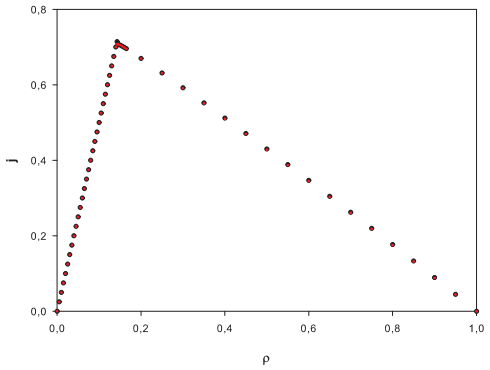

FIG. 3: Steady-state flux versus density for $p = 0.5$ and $L = 10^5$. Homogeneous and jammed ICs lead to identical stationary states except for a small interval of densities near maximum flux. Error bars are smaller than symbols.

Figure 3 shows the fundamental diagram obtained using homogeneous and jammed ICs for $p = 0.1$; for this value of p the stationary state is the same, regardless of the IC, except near $\rho = \frac{1}{7}$ where, for the homogeneous ICs, an absorbing configuration is attained, having a greater steady-state flux than obtained using jammed ICs. For higher probabilities p, we find a larger interval of densities in which the stationary behavior depends in the choice of IC. In Fig. 4, for $p = 0.5$, this interval corresponds to $0.118 \leq \rho \leq 0.143$; higher fluxes (black points) are obtained using homogeneous ICs, and lower fluxes (red) using jammed ICs. Homogeneous ICs rapidly evolve to an absorbing configuration, while jammed ICs, which feature a large initial activity, do not fall into an absorbing configuration for the duration of the simulation ($t_{max} = 10^7$), for the system size ($L = 10^5$) used here.

Systematic investigation of the steady-state flux obtained using homogeneous and jammed ICs leads to the conclusion that the ρ - p plane can be divided into three regions. To begin, we recall that for $\rho > \rho_c = 1/(v_{max} + 2)$ and $p > 0$, the mean velocity $\overline{v}$ must be smaller than v_{max}. Thus the activity is nonzero and the configuration (i.e., the set of values v_i and d_i) changes. In this region, homogeneous and jammed ICs always lead to the same steady state.

For $\rho < \rho_c$, absorbing configurations exist for any value of p. There is nevertheless a region with $\rho < \rho_c$ in which activity is long-lived. In this region, which we call the *active phase*, the steady state depends on whether the IC has little activity (homogeneous) or

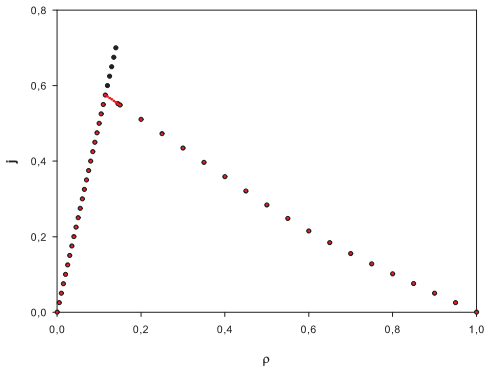

FIG. 4: Steady-state flux versus density as in Fig. 3, but for $p = 0.5$. Homogeneous and jammed ICs curves lead to identical stationary states except for densities near maximum flux.

much activity (jammed). Outside this region, all ICs evolve to an absorbing configuration; we call this the *absorbing phase*. The boundary between the active and absorbing phases, determined via the criterion of different steady states for homogeneous and jammed ICs, is shown in Fig. 5.

Our results are consistent with the following scenario, familiar from the study of phase transitions to an absorbing state [15–17]: for finite systems, all ICs with $\rho < \rho_c$ and $p > 0$ eventually fall into an absorbing configuration. Within the active phase, however, the mean lifetime of activity grows exponentially with system size. The phase boundary represents a line of critical points, on which the lifetime grows as a power law of system size. (Further details on critical behavior are discussed in Sec. IV.) A surprising feature of the phase boundary is that it is *reentrant*: for a given density in the range $0.116 < \rho < \rho_c$, the absorbing phase is observed for both small and large p values, and the active phase for intermediate values. The reason for this is discussed in Sec. III.C. We denote the upper and lower branches of the phase boundary by $p_+(\rho)$ and $p_-(\rho)$, respectively; they meet at $\rho_{c,<} \simeq 0.116$.

The phase boundary is singular at its small-p limit. As p tends to zero from positive values, the critical density approaches $1/7$, but for $p = 0$ the transition occurs at $\rho = 1/6$. The phase diagram of the ANS model for $0 < p < 1$ is similar to that of a stochastic sandpile [22, 23]. In the sandpile, there are no absorbing configurations for particle density $\rho > z_c - 1$, where z_c denotes the toppling threshold; nevertheless, the absorbing-state phase transition at a density strictly smaller than this value. Similarly, in the ANS model there are no absorbing configurations for $\rho > 1/7$, but the phase transition occurs at some smaller

density, depending on the deceleration probability p. Further parallel between the ANS model and stochastic sandpiles are noted below.

The phase boundary shown in Fig. 5 represents a preliminary estimate, obtained using the following criterion. Points along the lower critical line $p_-(\rho)$ correspond to the smallest p value such that each of 200 arbitrary ICs remain active during a time of 10^7 steps, in a system of $L = 10^5$ sites. Similarly, $p_+(\rho)$ corresponds to the largest p value such that all 200 realizations remain active. For selected points, a precise determination was performed, as described in Sec. IV. We defer a more precise mapping of the overall phase diagram to future work.

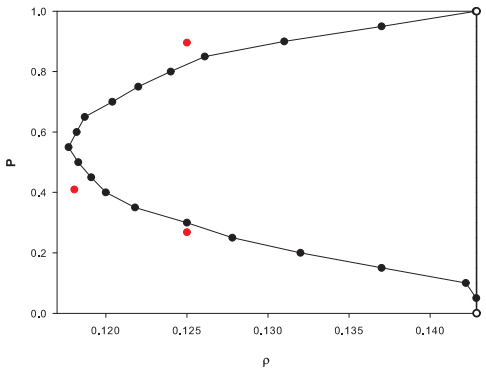

FIG. 5: Boundary between active and absorbing phases in the ρ - p plane. Black points: preliminary estimates from initial-condition dependence as explained in text. Red points: precise estimates obtained via finite-size scaling as described in Sec. IV. The open circle at $\rho = 1/7$, $p = 0$ is not part of the phase boundary: for $p = 0$ the transition occurs at $\rho = 1/6$. The open circle $\rho = 1/7$, $p = 1$ marks the other end of the phase boundary; we note however that at this point, all initial conditions evolve to the absorbing state.

The phase transitions at $p_-(\rho)$ and $p_+(\rho)$ appear to be continuous. (Indeed, discontinuous phase transitions between an active and an absorbing phase are not expected to occur in one-dimensional systems [19].) Figure 6 shows the steady-state activity (defined below) versus p for density $\rho = 1/8$. In the vicinity of the transition, the curves become sharper with increasing system size, as expected at a continuous phase transition to an absorbing state.

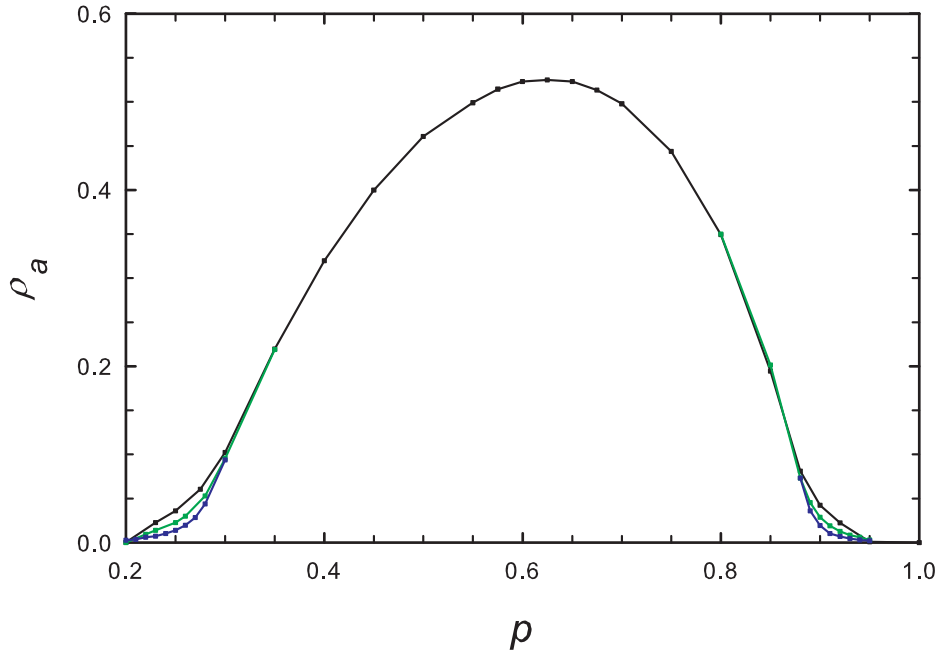

FIG. 6: Steady-state activity ρ_a versus p for vehicle density $\rho = 1/8$. System sizes $N = 1000$ (black), 2000 (green) and 4000 (blue). Error bars smaller than symbols.

B. Order parameter

Having identified a continuous absorbing-state phase transition in the ANS model, further analysis requires that we define an appropriate order parameter or activity density. Since the absorbing state is characterized by $v_i = v_{max}, \forall i$, one might be inclined to define the activity density simply as $\rho_a = v_{max} - \overline{v}$. The problem with this definition is that not all configurations with $v_i = v_{max}, \forall i$ are absorbing: a vehicle with $d_i = v_{max}$ may reduce its speed to $v_{max} - 1$, yielding activity in the first sense. Since such a reduction occurs with probability p, it seems reasonable to define the activity density as:

$$\rho_a = v_{max} - \overline{v} + p\rho_{a,2} \equiv \rho_{a,1} + p\rho_{a,2}, \tag{1}$$

where $\rho_{a,2}$ denotes the fraction of vehicles with $v_i = d_i = v_{max}$. According to this definition, the activity density is zero if and only if the configuration is absorbing, that is, if $v_i = v_{max}$, *and* $d_i > v_{max}$, $\forall i$. Studies of large systems near the critical point reveal that $\rho_{a,1} >> \rho_{a,2}$, so that the latter can be neglected in scaling analyses. It is nonetheless essential to treat configurations with $\rho_{a,2} > 0$ as *active*, even if $\rho_{a,1} = 0$.

C. Reentrance

In this subsection we discuss the reason for reentrance, that is, why, for $\rho_{c,<} < \rho < \rho_c$, the system reaches the absorbing state for *large* p as well as small p. Since deceleration is associated with generation of activity (i.e., of speeds $< v_{max}$), a reduction in activity as p tends to unity seems counterintuitive. The following intuitive argument helps to understand why this happens. For $p \simeq 0$, vehicles rarely decelerate if they have sufficient headway to avoid reaching the position of the car in front. This tends to increase the headway of the car behind, so that (for $\rho < \rho_c$), all headways attain values $\geq v_{max} + 1$, which represents an absorbing configuration. For $p = 1$, a car with speed $v_i = d_i$ always decelerates, which tends to increase its own headway. In either case, $p = 0$ or $p = 1$, as reduced headway (i.e., inter-vehicle intervals with $d_i < v_{max} + 1$) is transferred down the line, vehicles may be obliged to decelerate, until the reduced headway is transferred to an interval with headway d_i large enough that no reduction in velocity is required. [Intervals with $d_i > v_{max} + 1$, which we call *troughs*, always exist for $\rho < \rho_c = 1/(v_{max} + 2)$]. When all reduced headways are annihilated at troughs, the system attains an absorbing configuration.

Call events in which a vehicle having $v_i = d_i$ decelerates *D events*, and those in which such a vehicle does not decelerate *N events*. For $\rho < \rho_c$, if only D events (or only N events) are allowed, the system attains an absorbing configuration via annihilation of reduced headways with troughs. Thus some alternation between D and N events is required to maintain activity, and the active phase corresponds to intermediate values of p.

These observations are illustrated in Fig. 7, for a system of twenty vehicles with $v_{max} = 2$ and density $\rho = 2/9 < \rho_c = 0.25$. Initially, all vehicles have $v_i = v_{max}$. The headways d_i initially alternate between three and four (the latter are troughs), except for $d_{19} = 0$ and $d_{20} = 7$. In the left panel, for $p = 0$, the system reaches an absorbing configuration after four time steps. Similarly, in the right panel, for $p = 1$, an absorbing configuration is reached after 7 steps. For $p = 0.6$ (middle panel), the evolution is stochastic. Most realizations reach an absorbing configuration rapidly, but some remain active longer, as in the example shown here. From the distribution of D and N events, it appears that activity persists when vehicles first suffer an N event, reducing their own headway, and subsequently (one or two steps later) suffer a D event, reducing the headway of the preceding vehicle. Such an alternation of N and D events allows a region with reduced headways to generate more

activity before reaching a trough.

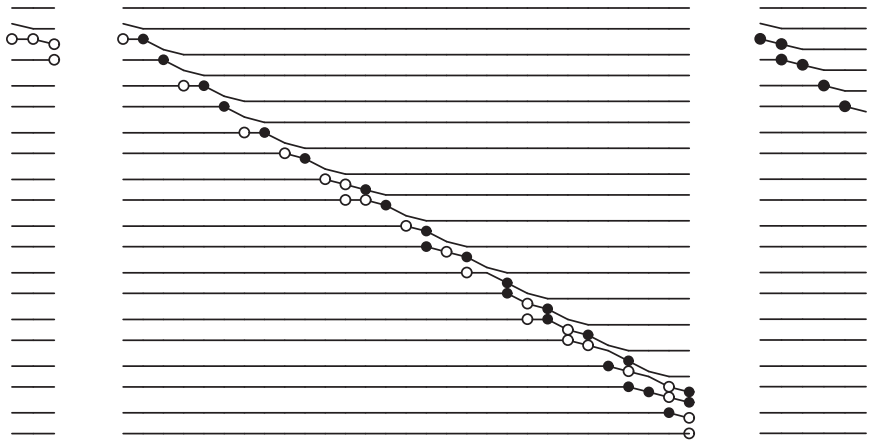

FIG. 7: Vehicle positions relative to the first (lowest) vehicle versus time t (horizontal) for $t \geq 2$, in a system with $N = 20$, $v_{max} = 2$ and vehicle density $\rho = 2/9 < \rho_c = 0.25$. Initially, all vehicles have $v_i = v_{max}$. The headways d_i initially alternate between three and four, except for $d_{19} = 0$ and $d_{20} = 7$. Filled (open) circles denote D (N) events, i.e., events in which a vehicle with speed $v_i = d_i$ decelerates (does not decelerate). In an absorbing configuration all velocities are equal, yielding a set of horizontal lines. Left panel: $p = 0$, system inactive for $t > 4$; right panel: $p = 1$, system inactive for $t > 7$; center panel: example of a realization with $p = 0.6$ in which activity persists until $t = 56$ (evolution for $t > 30$ not shown).

IV. CRITICAL BEHAVIOR

We turn now to characterizing the phase transition along the lines $p_-(\rho)$ and $p_+(\rho)$. Since the transition is continuous, this requires that we determine the associated critical exponents, in order to identify the universality class of the ANS model. The analysis turns out to be complicated by strong finite-size effects: different from simple systems exhibiting an absorbing-state phase transition, such as the contact process, for which studies of systems with $L \leq 1000$ yield good estimates for critical exponents [15], here we require systems of up to 10^5 sites to obtain reliable results. We are nevertheless able to report precise results at several points along the phase boundary.

We use quasistationary (QS) simulations to probe the behavior at long times conditioned

on survival of activity [18]. Since the deceleration probability p is continuous while the density ρ can only be varied in discrete steps, we keep the latter fixed and vary the former in each series of studies. As in other studies of QS behavior absorbing-state phase transitions, we focus on the finite-size scaling (FSS) of the activity density, ρ_a, the lifetime, τ, and the moment ratio $m = \langle \rho_a^2 \rangle / \rho_a^2$, as functions of system size, N [15, 18]. At a critical point, these variables are expected to exhibit scale-free (power-law) dependence on N, that is, $\rho_a \sim N^{-\beta/\nu_\perp}$ and $\tau \sim N^z$, where β is the order-parameter exponent and $\nu_\perp$ the exponent that governs the divergence of the correlation length as one approaches the critical point. In the active phase, ρ_a approaches a nonzero constant value, while τ grows exponentially as $N \to \infty$. In the absorbing phase, $\rho_a \sim 1/N$ while τ grows more slowly than a power law as $N \to \infty$. At the critical point, the moment ratio is expected to converge to a nontrivial limiting value, $m = m_\infty + \mathcal{O}(N^{-\lambda})$, with $\lambda > 0$. In the active (inactive) phase, m curves sharply downward (upward) when plotted versus $1/N$. These are the criteria we employ to determine the critical point, $p_c(\rho)$. The distance from the critical point can be estimated from the curvature of log-log plots of ρ_a and τ versus N.

As noted in Sec. III.B, the order parameter is the sum of two contributions: $\rho_a = \rho_{a,1} + p\rho_{a,2}$. In simulations, we therefore determine $\rho_{a,1}$ and $\rho_{a,2}$ separately. In the vicinity of the critical point we find $\rho_{a,1} \sim N^{-0.5}$ and $\rho_{a,2} \sim N^{-0.9}$, showing that the fraction $\rho_{a,2}$ of vehicles with $v_i = d_i = v_{max}$ decays more rapidly than $\rho_{a,1} = v_{max} - \overline{v}$, so that it makes a negligible contribution to the activity density for large N. We therefore adopt $\rho_{a,1}$ as the order parameter for purposes of scaling analysis. Configurations $\rho_{a,1} = 0$ and $\rho_{a,2} > 0$ are nevertheless considered to be active; only configurations with $v_i = v_{max}$ and $d_i > v_{max}$, $\forall i$, are treated as absorbing.

We study rings of 1000, 2000, 5000, 10 000, 20 000, 50 000 and 100 000 sites, calculating averages over a set of 20 to 160 realizations. Even for the largest systems studied, the activity density reaches a stationary value within 10^6 time steps. We perform averages over the subsequent 10^8 steps. As detailed in [18], the QS simulation method probes the quasistationary probability distribution by restarting the evolution in a randomly chosen active configuration whenever the absorbing state is reached. A list of N_c such configurations, sampled from the evolution, is maintained; this list is renewed by exchanging one of the saved configurations with the current one at rate p_r. Here we use $N_c = 1000$, and $p_r = 20/N$. During the relaxation phase, we use a value of p_r that is ten times greater, to eliminate the

vestiges of the initial configuration from the list. The lifetime τ is taken as the mean time between attempts to visit an absorbing configuration, in the QS regime.

Initial configurations are prepared by placing vehicles as uniformly as possible (for example, for density $\rho = 1/8$, we set $d_i = 7, \forall i$), and then exchanging distances randomly. In such an exchange a site j is chosen at random and the changes $d_j \to d_j - 1$ and $d_{j+1} \to d_{j+1} + 1$ are performed, respecting the periodic boundary condition, $d_{N+1} \equiv d_1$. The random exchange is repeated N_e times (in practice we use $N_e = 2N$), avoiding, naturally, negative values of d_j. Since headways $d_j < v_m$ are generated in this process, at the first iteration of the dynamics, velocities $v_j < v_{max}$ arise, leading to a relatively large, statistically uniform initial activity density.

We performed detailed studies for densities $\rho = 1/8$, on both the upper and lower critical lines, and for density $17/144 = 0.11805\overline{5}$, on the lower line. Figures 8, 9 and 10 show, respectively, the dependence of the order parameter, lifetime and moment ratio m on system size for density 1/8 and p values in the vicinity of the lower critical line. In the insets of Figs. 8 and 9 the values of ρ_a and τ are divided by the overall trend to yield $\rho_a^* \equiv N^{0.5}\rho_a$ and $\tau^* = \tau/N$. These plots make evident subtle curvatures hidden in the main graphs, leading to the conclusion that $p_c(\rho = 1/8)$ is very near 0.2683.

A more systematic analysis involves the curvatures of these quantities: we fit quadratic polynomials,

$$\ln \rho_a = \text{const.} + a \ln N + b(\ln N)^2, \tag{2}$$

and similarly for $\ln \tau$, to the data for the four largest system sizes. The coefficient of the quadratic term, which should be zero at the critical point, is plotted versus p in Fig. 11. Linear interpolation to $b = 0$ yields the estimates $p_c = 0.26830(3)$ (data for activity density) and $p_c = 0.26829(2)$ (data for lifetime); we adopt $p_c = 0.26829(3)$ as our final estimate. (Figures in parentheses denote statistical uncertainties.) The data for m, although more scattered, are consistent with this estimate: from Fig. 10 it is evident that p_c lies between 0.2681 and 0.2683.

To estimate the critical exponents $\beta/\nu_\perp$ and z we perform linear fits to the data for $\ln \rho_a$ and $\ln \tau$ versus $\ln N$ (again restricted to the four largest N values), and consider the slopes as functions of p. Interpolation to p_c yields the estimates: $\beta/\nu_\perp = 0.500(3)$ and

$z = 1.006(8)$. A similar analysis yields $m_c = 1.306(6)$. The principal source of uncertainty in these estimates is the uncertainty in p_c.

Using the data for ρ_a, τ and m we also estimate the critical exponent $\nu_\perp$. Finite-size scaling implies that the derivatives $|dm/dp|$, $d\ln\tau/dp$ and $d\ln\rho_a/dp$, evaluated at the critical point, all grow $\propto L^{1/\nu_\perp}$. We estimate the derivatives via least-squares linear fits to the data on an interval that includes p_c. (The intervals are small enough that the graphs show no significant curvature.) Power-law dependence of the derivatives on system size is verified in Fig. 12. Linear fits to the data for the four largest sizes, for $\ln\rho_p$, $\ln\tau$, and m yield $1/\nu_\perp = 0.494(15)$, $0.495(15)$, and $0.516(29)$, respectively, leading to the estimate $\nu_\perp = 2.00(5)$. Repeating the above analysis for simulations at vehicle density $\rho = 17/144$, we find $p_-(17/144) = 0.4096(1)$, $\beta/\nu_\perp = 0.503(6)$, $z = 1.011(15)$, $m = 1.302(2)$, and $\nu_\perp = 2.02(3)$.

Thus, for the two points studied on the lower critical line, the results are consistent with a simple set of exponent values, namely, $z = 1$, $\nu_\perp = 2$, and $\beta = 1$. The same set of critical exponents appears in a system of activated random walkers (ARW) on a ring, when the walkers hop in one direction only [20]. The critical moment ratio for ARW is $m_c = 1.298(4)$, quite near present estimates. We suggest that these values characterize a universality class of absorbing-state phase transitions in systems with a conserved density (of walkers in ARW, and of vehicles in the present instance), and anisotropic movement. The ARW with *symmetric* hopping is known to belong to the universality class of conserved directed percolation [21], which also includes conserved stochastic sandpiles [22, 23].

A study on the upper critical line for vehicle density $\rho = 1/8$ yields results that are similar but slightly different. Repeating the procedure described above, we find $p_+(1/8) = 0.89590(5)$, $\beta/\nu_\perp = 0.487(8)$, $z = 1.021(15)$, $\nu_\perp = 1.98(6)$, and $m_c = 1.315(5)$. The exponent values are sufficiently near those obtained on the lower critical line that one might attribute the differences to finite-size effects. We defer to future work more detailed analyses, to determine whether scaling properties along the upper and lower critical lines differ in any respect.

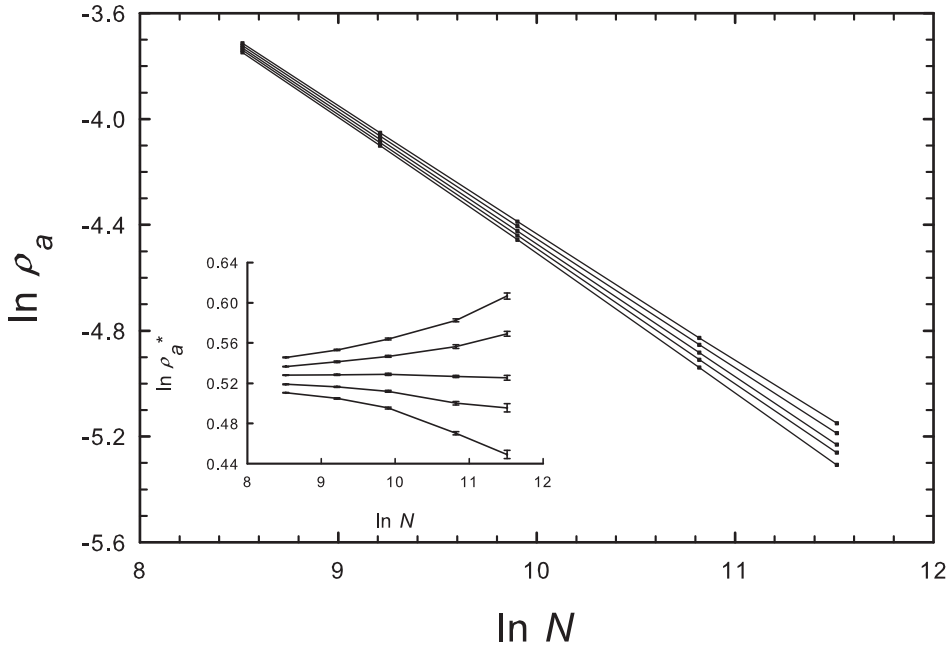

FIG. 8: Activity density versus number of vehicles for density 1/8 and (lower to upper) $p = 0.2679$, 0.2681, 0.2683, 0.2685 and 0.2687. Error bars are smaller than symbols. Inset: scaled activity density $\rho_a^* = N^{0.5}\rho_a$ versus number of vehicles.

V. SUMMARY

We consider a version of the Nagel-Schreckenberg model in which probabilistic deceleration is possible only for vehicles whose velocity is equal to the headway, $v_i = d_i$. In the resulting ANS model, a free-flow configuration, $v_i = v_{max}$ and $d_i > v_{max}$, $\forall i$, is *absorbing* for any value of the deceleration probability p. The phase transition in the original NS model at deceleration probability $p = 0$ is identified with the absorbing-state transition in the ANS model: the two models are identical for $p = 0$. In the original model, a nonzero deceleration probability corresponds to a spontaneous source of activity which eliminates the absorbing state, and along with it, the phase transition.

The ANS model, by contrast, exhibits a line of absorbing-state phase transitions in the ρ-p plane; the phase diagram is reentrant. We present preliminary estimates for the phase boundary and several critical exponents. The latter appear to be associated with a universality class of absorbing-state phase transitions in systems with a conserved density and asymmetric hopping, such as activated random walkers (ARWs) with particle transfer only

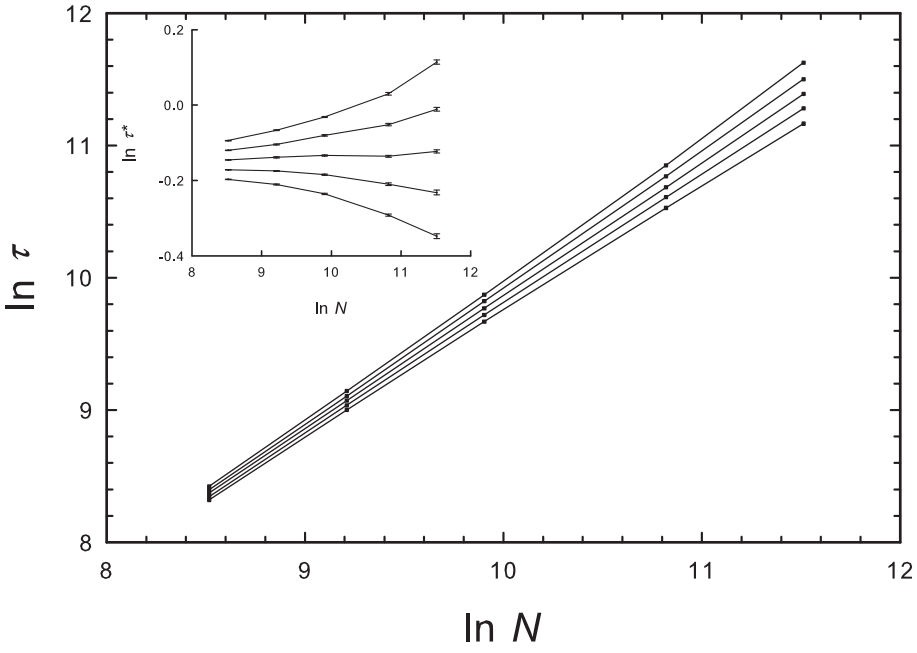

FIG. 9: Lifetime versus number of vehicles for density 1/8 and (lower to upper) $p = 0.2679$, 0.2681, 0.2683, 0.2685 and 0.2687. Error bars are smaller than symbols. Inset: scaled lifetime $\tau^* = N^{-1.0}\tau$ versus number of vehicles.

in one direction [20]. In this context it is worth noting that in traffic models, as well as in sandpiles and ARW, activity is associated with a local excess of density: in sandpiles, activity requires sites with an above-threshold number of particles; in ARW, it requires an active particle jumping to a site occupied by an inactive one; and in the ANS model, it requires headways d smaller than $v_{max}+1$. One may hope that the connection with stochastic sandpiles will lead to a better understanding of traffic models, and perhaps of observed traffic patterns.

Acknowledgments

This work was supported by CNPq and CAPES, Brazil.

[1] K. Nagel and M. Schreckenberg, "A cellular automaton model for freeway traffic," J. Phys. I (France) **2**, 221 (1992).

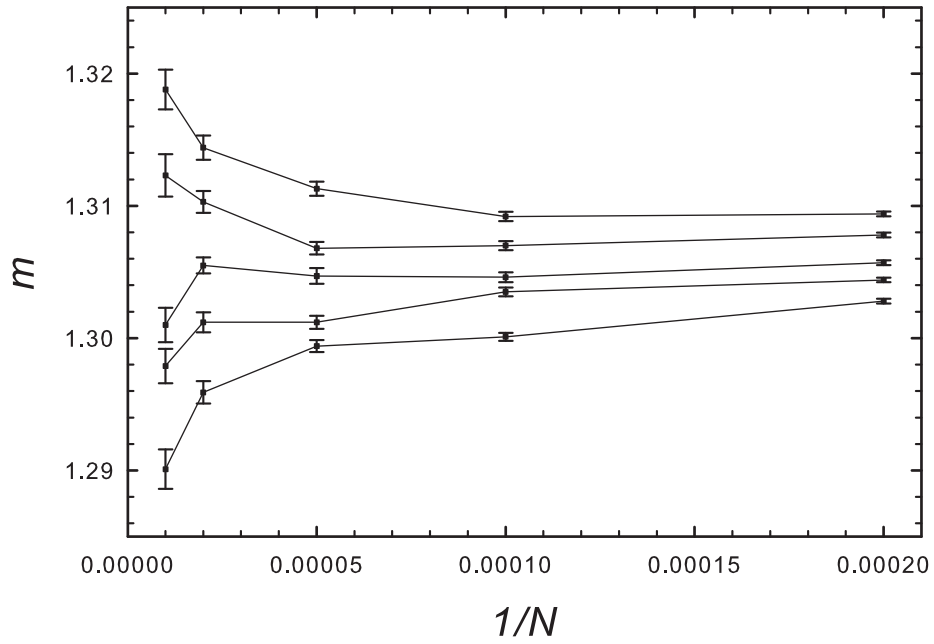

FIG. 10: Moment ratio m versus reciprocal system size for density 1/8 and (upper to lower) $p = 0.2679$, 0.2681, 0.2683, 0.2685 and 0.2687.

[2] G. Csányi and J. Kertész, "Scaling behaviour in discrete traffic models," J. Phys. A **28**, L427 (1995).

[3] B. Eisenblätter, L. Santen, A. Schadschneider, and M. Schreckenberg, "Jamming transition in a cellular automaton model for traffic flow," Phys. Rev. E **57**, 1309 (1998).

[4] M. Gerwinski and J. Krug, "Analytic approach to the critical density in cellular automata for traffic flow," Phys. Rev. E **60**, 188 (1999).

[5] A. M. C. Souza and L. C. Q. Vilar, "Traffic-flow cellular automaton: Order parameter and its conjugated field," Phys. Rev. E **80**, 021105 (2009).

[6] K. Nagel and M. Paczuski, "Emergent traffic jams," Phys. Rev. E **51** 2909 (1995).

[7] S. Krauss, P. Wagner, and C. Gawron, "Continuous limit of the Nagel-Schreckenberg model," Phys. Rev. E **54** 3707 (1996).

[8] M. Takayasu and H. Takayasu, "1/f noise in a traffic model," Fractals 1 **4** 860 (1993).

[9] S. C. Benjamin, N. F. Johnson, "Cellular automata models of traffic flow along a highway containing a junction," J. Phys. A **29** 3119 (1996).

[10] R. Barlovic, L. Santen, A. Schadschneider and M. Schreckenberg, "Metastable states in cellular

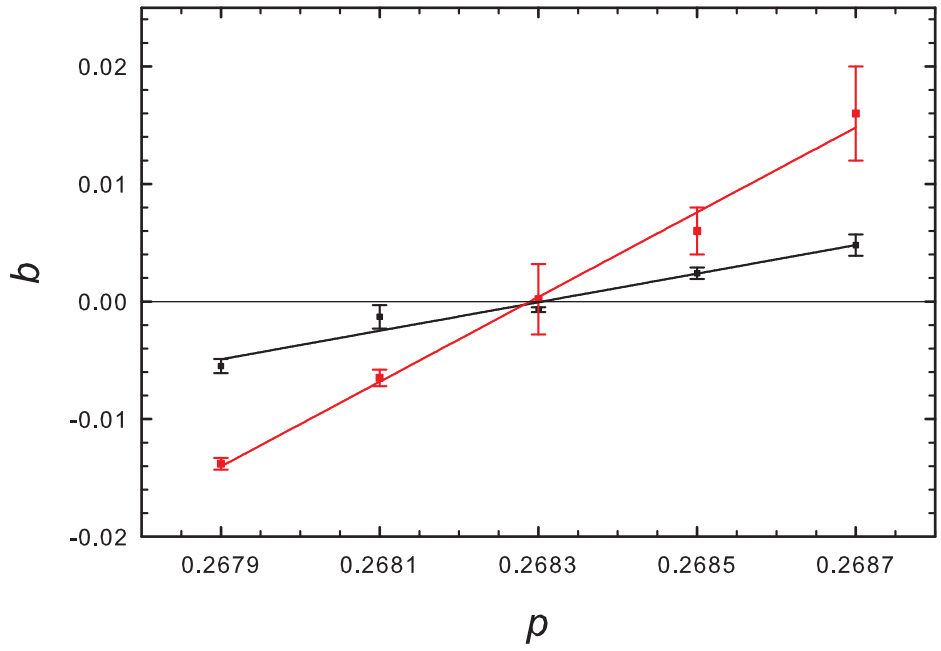

FIG. 11: (Color online) Curvature of $\ln \rho_a$ (black points) and $\ln \tau$ (red points) as functions of $\ln N$, as measured by the coefficient b of the quadratic term in least-squares quadratic fits to the data in Figs. 8 and 9. Straight lines are least-squares linear fits to b versus deceleration probability p, for vehicle density $\rho = 1/8$. Intercepts with the line $b = 0$ furnish estimates of p_c.

automata for traffic flow," Eur. Phys. J. B **5**, 793 (1998).

[11] S. Krauss, P. Wagner and C. Gawron, "Metastable states in a microscopic model of traffic flow," Phys. Rev. E **55**, 5597 (1997).

[12] X. Li, Q. Wu and R. Jiang, "Cellular automaton model considering the velocity effect of a car on the sucessive car," Phys. Rev. E **64**, 066128 (2001).

[13] A. Schadschneider, D. Chowdhury and K. Nishinari, *Stochastic Transport in Complex Systems from Molecules to Vehicles* (Elsevier, Oxford, 2011)

[14] P. Wagner and K. Nagel, "Comparing traffic flow models with different number of "phases"," Eur. Phys. J. B **63** 315 (2008).

[15] J. Marro and R. Dickman, *Nonequilibrium Phase Transitions in Lattice Models* (Cambridge University Press, Cambridge, 1999).

[16] G. Ódor, *Universality In Nonequilibrium Lattice Systems: Theoretical Foundations* (World Scientific, Singapore, 2007).

[17] M. Henkel, H. Hinrichsen and S. Lubeck, *Non-Equilibrium Phase Transitions Volume I: Ab-*

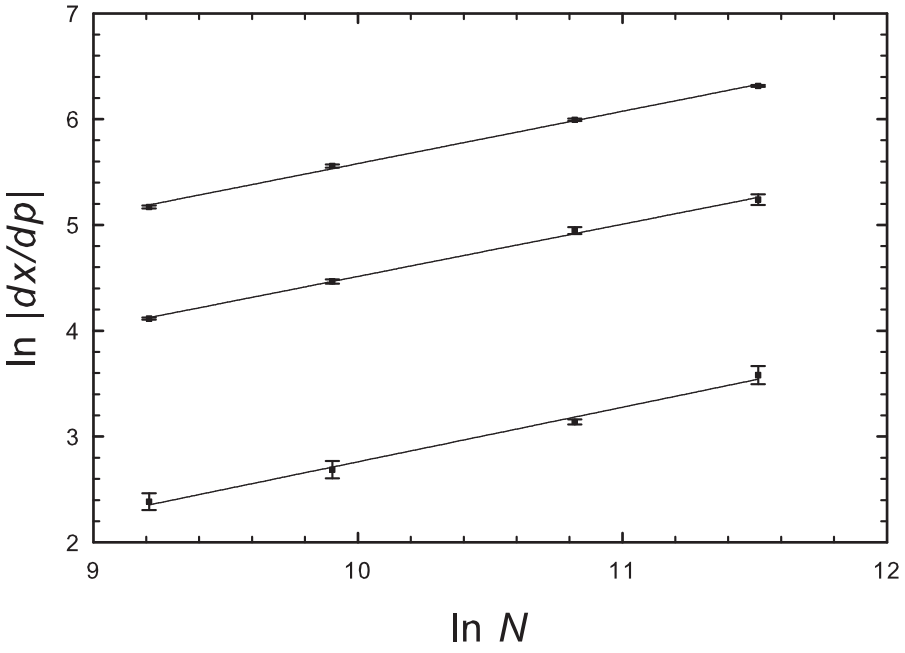

FIG. 12: Derivatives of (lower to upper) m, $\ln \rho_a$ and $\ln \tau$ with respect to p in the vicinity of p_c, versus N for vehicle density $\rho = 1/8$. Lines are least-squares linear fits to the data.

sorbing Phase Transitions (Springer-Verlag, The Netherlands, 2008).

[18] M. M. de Oliveira and R. Dickman, "How to simulate the quasistationary state," Phys. Rev. E **71**, 016129 (2005).

[19] H. Hinrichsen, "First-order transitions in fluctuating 1+1-dimensional nonequilibrium systems," eprint: cond-mat/0006212.

[20] R. Dickman, L. T. Rolla and V. Sidoravicius, "Activated Random Walkers: Facts, Conjectures and Challenges," J. Stat. Phys. **138**, 126 (2010).

[21] J. C. Mansur Filho and R. Dickman, "Conserved directed percolation: exact quasistationary distribution of small systems and Monte Carlo simulations," J. Stat. Mech. **2011**, P05029 (2011).

[22] M. A. Muñoz, R. Dickman, R. Pastor-Satorras, A. Vespignani, and S. Zapperi, "Sandpiles and absorbing-state phase transitions: recent results and open problems," in *Modeling Complex Systems*, Proceedings of the 6th Granada Seminar on Computational Physics, J. Marro and P. L. Garrido, eds., AIP Conference Proceedings v. 574 (2001).

[23] G. Pruessner, *Self-Organised Criticality*, (Cambridge University Press, Cambridge, 2012).